



OPEN

A novel hamster model of SARS-CoV-2 respiratory infection using a pseudotyped virus

Hiroshi Yamada¹, So-Ichiro Sasaki², Hideki Tani³, Mayu Somekawa¹, Hitoshi Kawasuji⁴, Yumiko Saga³, Yoshihiro Yoshida¹, Yoshihiro Yamamoto⁴, Yoshihiro Hayakawa² & Yoshitomo Morinaga¹✉

Severe acute respiratory syndrome coronavirus 2 (SARS-CoV-2) is a biosafety level (BSL)-3 pathogen; therefore, its research environment is limited. Pseudotyped viruses that mimic the infection of SARS-CoV-2 have been widely used for in vitro evaluation because they are available in BSL-2 containment laboratories. However, in vivo application is inadequate. Therefore, animal models instigated with animal BSL-2 will provide opportunities for in vivo evaluation. Hamsters (6–10-week-old males) were intratracheally inoculated with luciferase-expressing vesicular stomatitis virus (VSV)-based SARS-CoV-2 pseudotyped virus. The lungs were harvested 24–72 h after inoculation and luminescence was measured using an in vivo imaging system. Lung luminescence after inoculation with the SARS-CoV-2 pseudotyped virus increased in a dose-dependent manner and peaked at 48 h. The VSV-G (envelope G) pseudotyped virus also induced luminescence; however, a 100-fold concentration was required to reach a level similar to that of the SARS-CoV-2 pseudotyped virus. The SARS-CoV-2 pseudotyped virus is applicable to SARS-CoV-2 respiratory infections in a hamster model. Because of the single-round infectious virus, the model can be used to study the steps from viral binding to entry, which will be useful for future research on SARS-CoV-2 entry without using live SARS-CoV-2 or transgenic animals.

Severe acute respiratory syndrome coronavirus 2 (SARS-CoV-2) causes coronavirus disease 2019 (COVID-19) and has seriously affected our health and social activities. There is an urgent need to elucidate the pathophysiology of COVID-19 and to develop treatment and prophylactic approaches.

SARS-CoV-2 is classified as a biosafety level 3 (BSL-3) pathogen and requires a limited laboratory environment and strict control by skilled researchers¹. Research using live viruses has the advantage of evaluating disease pathogenicity more directly; however, there are some limitations in laboratories and efforts. Therefore, pseudotyped viruses, which are single-round infectious virus particles with an envelope protein originating from a different virus², have been widely used in COVID-19-related research because they can be used in BSL-2 containment laboratories. As an alternative to live SARS-CoV-2, we previously developed a pseudotyped virus, vesicular stomatitis virus (VSV), expressing luciferase, using the truncated spike (S) proteins of SARS-CoV-2³. The luminescence observed after treatment with luciferin reflected viral infection in cells and was highly infectious to humans (Huh7 and 293 T), hamsters (CHO), and monkeys (Vero)³. Pseudotyped viral systems have been widely used for in vitro evaluations, such as neutralization activity^{3–5}; however, whether they can also be used in animal models remains unknown.

SARS-CoV-2 uses angiotensin-converting enzyme 2 (ACE2) on the cell surface to bind to and enter cells. The SARS-CoV-2 S protein does not effectively bind to mouse ACE2⁶; therefore, sensitivity to infection is species-dependent. Thus, in vivo live virus infection models have been reported in SARS-CoV-2-sensitive animals, such as Syrian hamsters, transgenic mice expressing human ACE2, and ferrets⁷.

Animal models that can be instigated with Animal Biosafety Levels 2 (ABSL-2) will increase opportunities for in vivo evaluation. Therefore, in this study, a hamster model of SARS-CoV-2 respiratory infection using a VSV-based pseudotyped virus was established. Infectivity can be evaluated by in vivo imaging or quantification

¹Department of Microbiology, Graduate School of Medicine and Pharmaceutical Sciences, University of Toyama, 2630 Sugitani, Toyama 930-0194, Japan. ²Section of Host Defences, Institute of Natural Medicine, University of Toyama, Toyama, Japan. ³Department of Virology, Toyama Institute of Health, Toyama, Japan. ⁴Department of Clinical Infectious Diseases, Toyama University Graduate School of Medicine and Pharmaceutical Sciences, Toyama, Japan. ✉email: morinaga@med.u-toyama.ac.jp

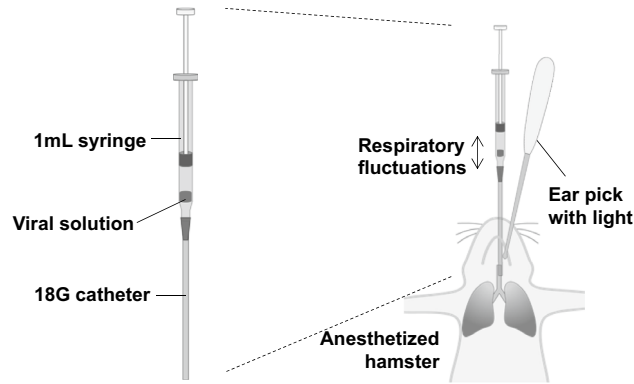


Figure 1. Schematic illustration of the inoculation of virus solution into the hamster airway. A viral solution (100 μ L/hamster) with a small amount of air was prepared in a 1 mL syringe attached to an 18G catheter. After observing the glottis of the anesthetized hamster with an ear pick with light, the syringe set containing the viral solution was inserted through the oral cavity and advanced through the vocal cords. The respiratory fluctuations of the viral solution indicated that the tip of the catheter was in the trachea.

of the VSV N gene expression. Because all procedures can be performed in BSL/ABSL-2 facilities, it expands the possibility of various ideas related to COVID-19 that could not be evaluated due to BSL3 limitations.

Materials and methods

Generation of pseudotyped viruses. Pseudotyped VSVs bearing SARS-CoV-2 S proteins were generated, as previously described³. The expression plasmid for the truncated S protein of SARS-CoV-2 and pCAG-SARS-CoV-2 S (hCoV-19/Japan/TY/WK-521/2020) was provided by Dr. Shuetsu Fukushi of the National Institute of Infectious Diseases, Japan. The S cDNA of SARS-CoV-2 with a 19 amino acid (aa) truncation at the C-terminus was cloned into the pCAGGS expression vector. Next, 293 T cells were grown to 80% confluence on collagen-coated tissue culture plates and transfected with each expression vector. After 24 h of incubation, cells transfected with each plasmid were infected with G-complemented (*G) VSV Δ G/Luc (*G-VSV Δ G/Luc) at a multiplicity of infection (MOI) of 0.5 per cell. After 24 h of incubation, the culture supernatants containing pseudotyped VSVs were centrifuged and stored at -80°C until ready for use. Pseudotyped VSVs bearing envelopes (G) (VSV-G) were also generated. The pseudotyped VSVs were stored at -80°C until subsequent use. Finally, VeroE6/TMPRSS2 cells (JCRB1819) were infected with the viral solution, the fluorescence level was measured, and the concentration of the solution was adjusted to approximately 5×10^4 – 5×10^5 RLU/ μ L for in vivo experiments (onefold concentration).

Animals. All experiments and methods were performed in accordance with the relevant guidelines and regulations. All experimental protocols used in this study were approved by the Animal Care and Use Committee of the University of Toyama (Protocol Number: A2020MED-18). Experiments and analyses were performed according to the ARRIVE guidelines.

Hamster models. Six-to-10-week-old male hamsters were purchased from Japan SLC Inc. (Shizuoka, Japan). All animals were housed in a pathogen-free environment in the Division of Animal Resources and Development at the University of Toyama.

After titration of the viral solution, 100 μ L (7.1×10^5 – 10^6 RLU/hamster for SARS-CoV-2 pseudotyped virus [SARS-CoV-2pv] and 7.1×10^7 – 10^8 RLU/hamster for VSV-G pseudotyped virus [VSV-Gpv]) were directly inoculated into the trachea, as previously described⁸. Briefly, after anesthesia with isoflurane or a mixture of medetomidine (0.15 mg/kg), midazolam (2 mg/kg), and butorphanol (2.5 mg/kg), viral solutions were administered through the trachea using an 18 G (65 mm long) catheter (TOP Co., Tokyo, Japan) with a 1 mL syringe under the assistance of an ear pick with light (Fig. 1). Immediately after confirming that the solution in the syringe showed respiratory fluctuations, the viral solution was administered to the lower respiratory tract.

Bioluminescent imaging. The hamsters were sacrificed using isoflurane and cervical dislocation 24 h after infection. The lungs were harvested and washed with phosphate-buffered saline (Nakarai Tesque, Kyoto, Japan). The lungs were incubated with 1 mg/mL of D-luciferin (Promega, Madison, WI, USA) for 5 min, and luminescence was measured using an in vivo imaging system (IVIS Lumina II, Perkin Elmer, MA, USA). Analyses were performed using Living Image 4.2 software (Caliper Life Science) to measure the light emitted from the infection sites. Luminescence from the front and back of the lungs was measured and the sum was calculated. All values are expressed as photons per second per cm^2 per steradian (p/sec/ cm^2 /sr) for each hamster.

Quantification of VSV N expression. To evaluate viral infection, VSV N gene expression in the lungs was measured by quantitative polymerase chain reaction⁹. The lungs were homogenized in a tube containing glass beads and 500 μ L of pre-chilled phosphate-buffered saline using BeadMill 24 (Thermo Fisher Scientific,

MA) at a speed of 6 m/s for 60 s. Each 20 μL of homogenized lung solution was immediately mixed with 500 μL of Isogen (Nippon Gene, Toyama, Japan) and stored at $-80\text{ }^{\circ}\text{C}$ until subsequent use. Total RNA was extracted using a QIAamp Viral RNA Mini Kit (Qiagen, Hilden, Germany), according to the manufacturer's instructions. Total RNA was reverse-transcribed into cDNA and then amplified using Thunderbird SYBR qPCR/RT Set III (TOYOBO Co., Tsuruga, Japan). VSV N expression was normalized to that of γ -actin¹⁰.

Statistical analysis. The luminescence data are expressed as the mean \pm standard error of the mean (SEM). Differences between low and high SARS-CoV-2pv concentrations were examined for statistical significance using an unpaired Student's t-test with GraphPad Prism version 8.4.3 (GraphPad Software, CA, USA). Because high values for higher SARS-CoV-2pv concentrations were expected, a one-tailed P value of <0.05 denoted the presence of a statistically significant difference.

Results

Intratracheal inoculation of SARS-CoV-2 pseudotyped virus demonstrated signs of lung infection. To develop a SARS-CoV-2 pseudotyped viral infection model, we first inoculated VSV-Gpv or SARS-CoV-2pv intranasally; however, no luminescence was observed by bioluminescent imaging (data not shown). Thus, the viral solutions were inoculated intratracheally (Fig. 1). Inoculation with VSV-Gpv or SARS-CoV-2pv induced no clinical signs until 24 h after inoculation.

For VSV-Gpv, no luminescence was detected in the lungs inoculated with 7.1×10^6 RLU/hamster (one-fold concentration; data not shown). Thus, higher concentrations of VSV-Gpv (10- and 100-fold) were inoculated (Fig. 2A). The luminescence values of the 10- and 100-fold concentrations were $0.16 \pm 0.08 \times 10^7$ and $2.8 \pm 0.88 \times 10^7$ p/sec/cm²/sr, respectively ($p < 0.05$, $n = 3$ each) (Fig. 2B).

In contrast, luminescence was clearly observed when 7.1×10^6 RLU SARS-CoV-2pv was inoculated (Fig. 2A). The mean \pm SEM of the luminescence values after inoculation of 7.1×10^5 RLU/hamster (0.1-fold concentration) and 7.1×10^6 RLU/hamster (onefold concentration) were $0.35 \pm 0.11 \times 10^7$ and $2.80 \pm 1.8 \times 10^7$ p/sec/cm²/sr, respectively ($p < 0.05$, $n = 3$ each) (Fig. 2B). The viral loads in the lungs increased in a dose-dependent manner in the VSV-Gpv and SARS-CoV-2pv inoculated hamsters (Fig. 2C).

Thus, luminescence values and viral loads reflected the amount of VSVGpv inoculated.

Signals of SARS-CoV-2 pseudotyped virus lung infection peaked at 48 h after inoculation. To confirm the time course of the model, luminescence levels and viral loads were measured until 72 h after inoculation. The luminescence values peaked 48 h after inoculation and then decreased to the same level as that 24 h after inoculation (Fig. 3A). The viral loads in the lungs also peaked at 48 h after inoculation and then slightly decreased at 72 h (Fig. 3B).

These results indicate that VSV-Gpv infection persisted for up to 48 h with increasing signals.

Discussion

Our results demonstrated that VSV-based SARS-CoV-2pv was applicable to SARS-CoV-2 respiratory infection in the hamster model. This method could be used as an alternative model for experiments in an ABSL-3 facility or to avoid handling highly infectious viruses, and it expands the possibility of analysis by using equipment that cannot be used with BSL-3/ABSL-3.

A lower respiratory infection model using pseudotyped SARS-CoV-2 has not been reported to date. Although a mouse model using lentivirus-based SARS-CoV-2pv following intranasal administration of human ACE2 has been reported¹¹, the virus did not infect the lower respiratory tract and remained around the nose. Generally, nasal inoculation is a convenient route for inducing lower respiratory tract infections. However, in our preliminary experiments, sufficient luminescence was not observed by *in vivo* imaging after nasal inoculation with the pseudotyped virus (data not shown). Therefore, it is essential to approach the lower respiratory tract directly. A tracheostomy approach from the anterior neck is a possible inoculation route for pathogens into the lower respiratory tract¹²; however, our intratracheal approach is less invasive and complicated. Confirmation of respiratory fluid fluctuations provided good reproducibility of the models. The time required for inoculation was approximately 1–3 min per hamster.

Our model can be used for research on the viral binding steps. For example, it would be useful in research on the treatment and prevention of viral binding and entry. However, this model is unsuitable for assessing advanced status, such as severe conditions and extrapulmonary infections, because of the single-round infectious virus. Because the viral solution was sprayed blindly, the infected lesion might have been one-sided, and it was better to evaluate both the front and back sides. The imaging findings were consistent with VSV N expression, suggesting that *in vivo* imaging is a suitable assay for evaluating the viral load. In the present study, despite inoculation with the same infectivity VSV-Gpv *in vitro*, an approximately 100-fold concentration was required to show relative luminescence *in vivo*. This finding could be a result of the expression ratios of the low-density lipoprotein receptor used by VSV¹³, and the ACE2 receptor used by SARS-CoV-2 differing *in vitro* and *in vivo*. However, VSV-Gpv could be used as a control in intervention studies by inoculating with a 100-fold dose if required.

The model can be useful as an assessment model for the evaluation of treatment interventions, such as antiviral drugs or antibodies, for at least 24 to 48 h. The appropriate time for the evaluation depends on the intervention; however, it could be easy to obtain data with good reproducibility until 48 h. On the other hand,

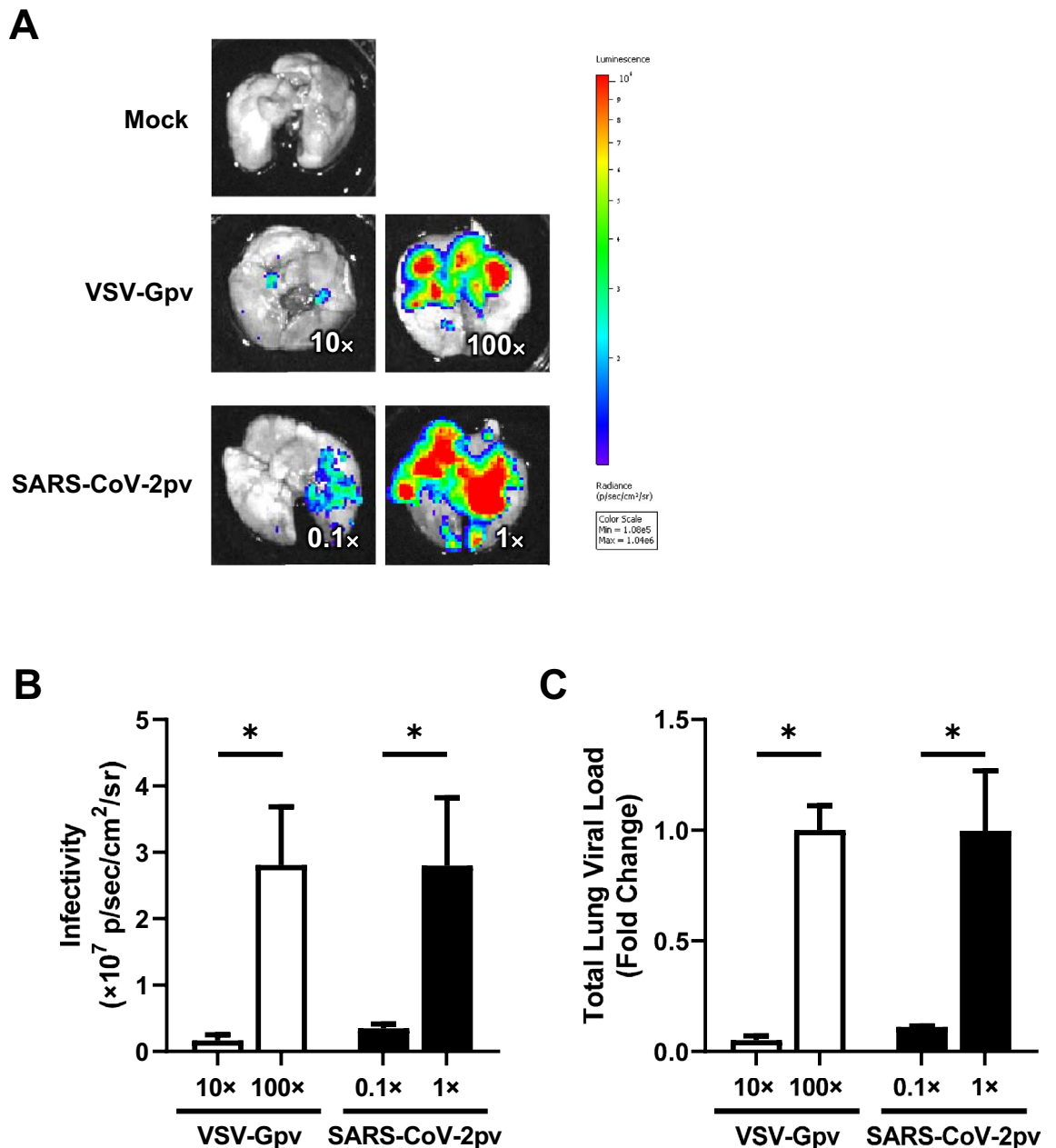


Figure 2. Dose-dependent infectivity after inoculation of the pseudotyped virus. (A) Representative lung imaging after inoculation of mock (top), VSV-Gpv (middle), and SARS-CoV-2pv (bottom). The numbers indicate the concentration ratio from the original viral solution (7.1×10^6 RLU/hamster). (B) Infectivity after inoculation of VSV-Gpv ($n=3$) and SARS-CoV-2pv ($n=3$). Data are expressed as the mean of sum luminescence of the front and back. (C) Viral loads in lungs evaluating VSV N expression. Data are expressed as the fold change from the higher concentration (VSV-Gpv; $n=2$, SARS-CoV-2pv; $n=3$). All experiments were performed 24 h after inoculation. Error bars are the SEM. * indicates $p < 0.05$.

because the natural decline in luminescence levels and viral loads was observed at 72 h, it could be inappropriate for treatment evaluation.

In conclusion, we successfully established a hamster model of SARS-CoV-2 respiratory infection by using a VSV-based pseudotyped virus. This model can be used to evaluate treatment and preventive potential without using highly infective pathogens and transgenic animals. As it is not limited to ABSL-3 containment, further studies can evaluate different ideas, which will be useful for future COVID-19 studies.

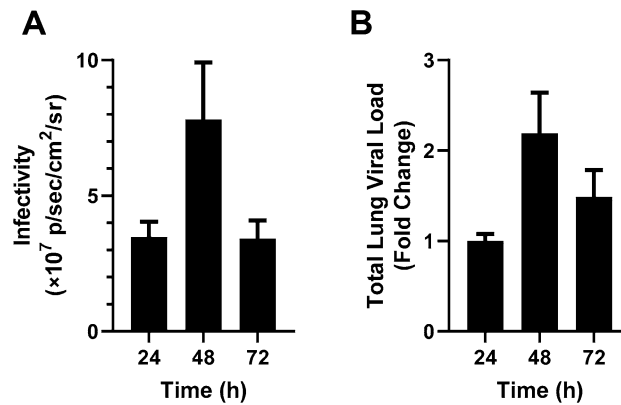


Figure 3. Time course of infectivity after inoculation of the pseudotyped virus. **(A)** Time course of luminescence levels after inoculation of SARS-CoV-2pv (n = 3, each). Data are expressed as the mean of sum luminescence of the front and back. **(B)** Time course of viral loads in lungs (n = 3, each). Data are expressed as the fold change from the higher concentration.

Data availability

There is no additional data.

Received: 25 November 2021; Accepted: 21 June 2022

Published online: 01 July 2022

References

1. Yeh, K. B. *et al.* Significance of high-containment biological laboratories performing work during the COVID-19 pandemic: Biosafety level-3 and -4 labs. *Front. Bioeng. Biotechnol.* **9**, 720315. <https://doi.org/10.3389/fbioe.2021.720315> (2021).
2. King, B. *et al.* Technical considerations for the generation of novel pseudotyped viruses. *Fut. Virol.* **11**, 47–59 (2016).
3. Tani, H. *et al.* Evaluation of SARS-CoV-2 neutralizing antibodies using a vesicular stomatitis virus possessing SARS-CoV-2 spike protein. *Virol. J.* **18**, 16. <https://doi.org/10.1186/s12985-021-01490-7> (2021).
4. Xie, X. *et al.* Neutralization of SARS-CoV-2 spike 69/70 deletion, E484K and N501Y variants by BNT162b2 vaccine-elicited sera. *Nat. Med.* **27**, 620–621. <https://doi.org/10.1038/s41591-021-01270-4> (2021).
5. Gaebler, C. *et al.* Evolution of antibody immunity to SARS-CoV-2. *Nature* **591**, 639–644. <https://doi.org/10.1038/s41586-021-03207-w> (2021).
6. Zhou, P. *et al.* A pneumonia outbreak associated with a new coronavirus of probable bat origin. *Nature* **579**, 270–273. <https://doi.org/10.1038/s41586-020-2012-7> (2020).
7. Muñoz-Fontela, C. *et al.* Animal models for COVID-19. *Nature* **586**, 509–515. <https://doi.org/10.1038/s41586-020-2787-6> (2020).
8. Morinaga, Y. *et al.* Exploring the microbiota of upper respiratory tract during the development of pneumonia in a mouse model. *PLoS ONE* **14**, e0222589. <https://doi.org/10.1371/journal.pone.0222589> (2019).
9. Zhang, X. *et al.* Mucin-like domain of ebola virus glycoprotein enhances selective oncolytic actions against brain tumors. *J. Virol.* **94**, 1. <https://doi.org/10.1128/jvi.01967-19> (2020).
10. Espitia, C. M. *et al.* Duplex real-time reverse transcriptase PCR to determine cytokine mRNA expression in a hamster model of New World cutaneous leishmaniasis. *BMC Immunol.* **11**, 31. <https://doi.org/10.1186/1471-2172-11-31> (2010).
11. Tseng, S. H. *et al.* A novel pseudovirus-based mouse model of SARS-CoV-2 infection to test COVID-19 interventions. *J. Biomed. Sci.* **28**, 34. <https://doi.org/10.1186/s12929-021-00729-3> (2021).
12. Hong, W. *et al.* A mouse model for SARS-CoV-2-induced acute respiratory distress syndrome. *Signal Transduct. Target. Ther.* **6**, 1. <https://doi.org/10.1038/s41392-020-00451-w> (2021).
13. Finkelshtein, D., Werman, A., Novick, D., Barak, S. & Rubinstein, M. LDL receptor and its family members serve as the cellular receptors for vesicular stomatitis virus. *Proc. Natl. Acad. Sci. USA* **110**, 7306–7311. <https://doi.org/10.1073/pnas.1214441110> (2013).

Acknowledgements

We would like to thank Makito Kaneda and Yushi Murai for their assistance with anesthesia and euthanasia. We also gratefully acknowledge Ms. Yumiko Nakagawa for her secretarial assistance.

Author contributions

Conceptualization: H.T., Y.M.; Methodology: H.T., Y.M.; Validation: H.T., Y.M.; Formal Analysis: Y.M.; Investigation: H.Y., M.S., Y.Yo., Y.M. (animal model); S.S., Y.H. (in vivo imaging); Resources: H.T., Y.S. (generating pseudotyped viruses); Data Curation: H.Y., Y.M.; Writing—Original Draft Preparation: H.Y., H.T., Y.M.; Writing—Review and Editing All authors; Visualization: H.Y., S.S.; Supervision: H.T., Y.Ya., Y.M.; Project Administration: Y.M.; Funding: H.T., Y.Ya., Y.M.

Funding

This study was supported by the Research Program on Emerging and Re-emerging Infectious Diseases from AMED Grant No. JP20he0622035 (HT, YYa, and YM), and the Research Funding Grant by the President of the University of Toyama (YYa, and YM).

Competing interests

The authors declare no competing interests.

Additional information

Correspondence and requests for materials should be addressed to Y.M.

Reprints and permissions information is available at www.nature.com/reprints.

Publisher's note Springer Nature remains neutral with regard to jurisdictional claims in published maps and institutional affiliations.



Open Access This article is licensed under a Creative Commons Attribution 4.0 International License, which permits use, sharing, adaptation, distribution and reproduction in any medium or format, as long as you give appropriate credit to the original author(s) and the source, provide a link to the Creative Commons licence, and indicate if changes were made. The images or other third party material in this article are included in the article's Creative Commons licence, unless indicated otherwise in a credit line to the material. If material is not included in the article's Creative Commons licence and your intended use is not permitted by statutory regulation or exceeds the permitted use, you will need to obtain permission directly from the copyright holder. To view a copy of this licence, visit <http://creativecommons.org/licenses/by/4.0/>.

© The Author(s) 2022